EXTENSION OF THE ESA TOOL FOR TRACKING THE HEALTH OF THE ENVIRONMENT AND MISSIONS IN SPACE

Camilla Colombo[(1)], Martina Rusconi[(1)], Juan Luis Gonzalo[(1)(2)], Wiebke Retagne[(1)], Andrea Muciaccia[(1)], Francisco J. Simarro Mecinas[(3)], Diego Ramirez[(3)], Francesca Letizia[(4)], Emma Stevenson[(4)]

(1) Politecnico di Milano, Via La Masa 34, 20133 Milan, Italy, Email: camilla.colombo@polimi.it; martina.rusconi@polimi.it; wiebke.retagne@polimi.it; andrea.muciaccia@polimi.it
(2) Currently at Universidad Rey Juan Carlos, Camino del Molino 5, 28943 Fuenlabrada (Madrid), Spain, Email: juan.gonzalo@urjc.es
(3) GMV, Email: fjsimarro@gmv.com; dramirez@gmv.com
(4) European Space Agency, Keplerlaan 1, Noordwijk, 2201 AZ, The Netherlands, Email: Francesca.Letizia@esa.int; Emma.Stevenson@ext.esa.int

ABSTRACT

The solution to the space debris problem requires a coordinated action to evaluate the current overall space carrying capacity and the contribution that each mission apports to it. The THEMIS software for "Tracking the Health of the Environment and Missions in Space" can be used to assess the impact of a space mission on the space debris environment. Sensitivity analyses are performed to assess the influence of the software settings on the index computation. The resulting effect maps and index values are then compared. Then, the design of the implementation changes for THEMIS 2.0 are described and the Beta testing phase is presented and kicked off.

1 INTRODUCTION

The solution to the space debris problem requires a coordinated action to evaluate the current overall space carrying capacity and the contribution that each mission apports to it. The THEMIS software for "Tracking the Health of the Environment and Missions in Space" can be used to assess the impact of a space mission on the space debris environment. This is measured in terms of risk based on the probability of the newly launched objects fragmenting or exploding during its mission, and the resulting effect on the overall population of active satellites. This debris indicator can be then used for evaluating possible mission design options in terms of orbit selection, and spacecraft characteristics. When the THEMIS index of each active object in the population of active satellites is aggregated, it is used as a measure of the overall used space capacity. This metric can be exploited to compare various future scenarios of the evolution of the space environment and evaluate the risk of operating in a specific orbital slot.

This paper presents the advancements on the THEMIS software, carried out as part of the activity *"*S2-SD-02 - Extended Methods for Space Debris Consequence and Space Capacity Analyses*"* funded by the European Space Agency through the Space Safety programme. The project aims at deploying the frontend of the software for use by the space community (e.g., space operators, spacecraft manufacturers, regulators and space debris experts). As part of the first task of the project, sensitivity analyses are performed to assess the influence of the software settings on the index computation. Some of the parameters analysed affect the computation of the severity part of the risk index, such as the time of propagation of the fragments cloud caused by a potential fragmentation of the object in orbit, and the definition of the representative targets' population affected by the fragmentation. Others influence the collision and explosion probabilities of the object, such as the limit on trackability for small debris fragments (which affects the feasibility of implementing collision avoidance manoeuvres to protect from them), the minimum threshold on debris' size to have catastrophic fragmentations, and post-mission disposal design options for the mission. The resulting effect maps and index values are then compared to analyse how the peaks of highest collision risk move for different settings, how the different effect maps influence ranking of objects in orbit and how the evolution of the index for some selected missions changes accordingly. These modifications are analysed to discuss what are the physical explanations behind them and to understand which settings should be chosen for different application of the space debris index.

As part of the second task, the gaps in the software and the user stories to be further implemented in an Agile approach are defined. The first set of user stories tackles the increase of applicability of the tool, the augmentation of the efficiency in terms of computational time and memory storage, and the integration of the software with the ESA Debris Mitigation Facility. Finally, the Beta testing phase of the THEMIS software is going to be presented and kicked off.

2 SENSITIVITY AND CONFIGURATION OPTIONS ANALYSIS

A sensitivity and configuration options analysis is

Proc. 9th European Conference on Space Debris, Bonn, Germany, 1–4 April 2025, published by the ESA Space Debris Office
Editors: S. Lemmens, T. Flohrer & F. Schmitz, (http://conference.sdo.esoc.esa.int, April 2025)

performed with the goal of assessing the impact of some default choices in the modelling and computation of the debris index. Several analyses have been performed, namely:

- Impact of the time of debris cloud propagation on the effect maps and single mission index value.
- Impact of the time of debris cloud propagation on the ranking of in-space objects.
- Impact of including the Starlink constellation in the target population.
- Impact of the upper cap for the ejection velocity of fragments in the case of catastrophic collisions on the effect maps.
- Different criteria for updating the targets population.
- Different approaches to define the threshold for observable debris size for lethal non-trackable objects.
- Different post mission disposal re-entry strategies, among which: direct re-entry, targeted disposal, re-orbit, and no disposal, on the value of the mission index [1],[2]
- Impact of the time step for saving the density snapshots on the effect maps.

This paper will focus only on the sensitivity analysis on the time of debris cloud propagation and its impact on the effect maps and the population ranking. Moreover, the impact of including in the target population the Starlink constellation is also evaluated. The other analyses will be presented in a future work [3].

As described in [1],[2],[4],[5],[6] the evaluation of the impact of a space mission on the space debris environment is done through a risk metric that computes the risk of collision and explosion of a single mission through its lifetime and the consequent effect that such a fragmentation event would have on the current population of active object. The space debris index in THEMIS follows the formulation of the Environmental Consequences of Orbital Breakups (ECOB) index [7] and is defined as a risk indicator. The formulation is composed by a probability term (p), which quantifies the collision probability due to the space debris background population and the explosion probability of the analysed object, and a severity term (e) associated to the effects of the fragmentation of objects in a given orbital region. The index evaluation at a single time epoch is computed as

$$I = p_c \cdot e_c + p_e \cdot e_e \tag{1}$$

where p_c and p_e represent the collision and explosion probabilities, and e_c and e_e represent the collision and explosion effects, respectively.

The effect term of the index is calculated by triggering and propagating synthetic debris clouds in each bin of a grid in orbital elements. The choice of the orbital elements to be considered for the fragmentation grid depends on the region under analysis, i.e., Low Earth Orbit (LEO), (low or high) Medium Earth Orbit (MEO), Geostationary Earth Orbit (GEO) or GEO Transfer Orbit (GTO); however, the generated cloud is propagated in all the elements. The effect of each fragment cloud is then assessed against a population of representative targets that are chosen to represent the snapshot of active missions in space at a reference given epoch. For example, the representative targets for the LEO population are defined in a grid in semi-major axis, a, and inclination, i, (with a step of 25 km and 5 degrees) since they are considered as the main design parameters for missions in LEO and the most representative elements from a dynamical point of view. A range of a of [6771, 8371] km and i of [0, 180] degrees is considered [4]. The computation of the effect term both for collisions and explosions is carried out in three steps:

1. Estimation of the initial fragments' density distribution, through a probabilistic reformulation of the NASA Standard Breakup Model [8].
2. Propagation of the fragments' density through the Method Of Characteristics (MOC), and consequent characteristics' interpolation through binning in the 7D phase space of Keplerian elements and area-to-mass ratio implemented in the Starling 2.0 software [9].
3. Evaluation of the cumulative number of impacts of the cloud against each representative target over the considered time frame [10]. The representative targets' cross-sectional area is assumed to be unitary since the result is rescaled a posteriori.

2.1 Impact of the time of debris cloud propagation on the effect maps

In the THEMIS 1.0 software, by default, the debris cloud originating in each bin is propagated by Starling 2.0 over a 15-year period as in [7], with density snapshots saved annually. The effect term is computed as the cumulative collision or explosion probability over the entire 15-year period. Two possible formulations exist, one formulation compute the effect as:

$$e = \frac{1}{\boldsymbol{A_{TOT}}} \sum_{i=1}^{N_t} P_{c_i}(\Delta t = 15\text{ ys})\, A_i \tag{2}$$

where A_{TOT} is the overall cross-sectional area of the representative objects in the population, A_i is the cumulative cross-section of the objects belonging to the i^{th} bin, and P_{c_i} is the collision probability for the bin. The second formulation instead compute the effect as:

$$e = \frac{1}{\boldsymbol{A_{TOT_0}}} \sum_{i=1}^{N_t} P_{c_i}(\Delta t = 15\text{ ys})\, A_{t_i} \tag{3}$$

that with respect to the ECOB formulation in [7] changes the denominator by considering the cumulative cross-sectional area in the bins hosting a target at a reference epoch A_{TOT_0}, rather than at the analysis epoch. In both Eqs. (2) and (3)

$$P_{c_i} = 1 - e^{-\emptyset \cdot A_i \cdot \Delta t} \quad (4)$$

with $\emptyset$ the debris flux in 1/km^2/year, A_i is the average cross-sectional area in the i-th bin, t is the time considered in years, A_{t_i} is the total cross-sectional area of the i-th bin.

The current results use the formulation in Eq (2). To assess the impact of different propagation times, the debris clouds are initially propagated for a maximum time of 100 years and then the number of impacts and the effect maps are computed over [1, 5, 10, 15, 25, 50, 100] years. To emphasise the impact of large constellations on the resulting maps, the results of the analysis are presented both with and without the inclusion of the Starlink constellation in the population of representative targets. Figure 1 shows the collision effect maps in LEO for different times of debris cloud propagation. The white dots are representative targets positions, not including (left column) and including the Starlink constellation (right column).

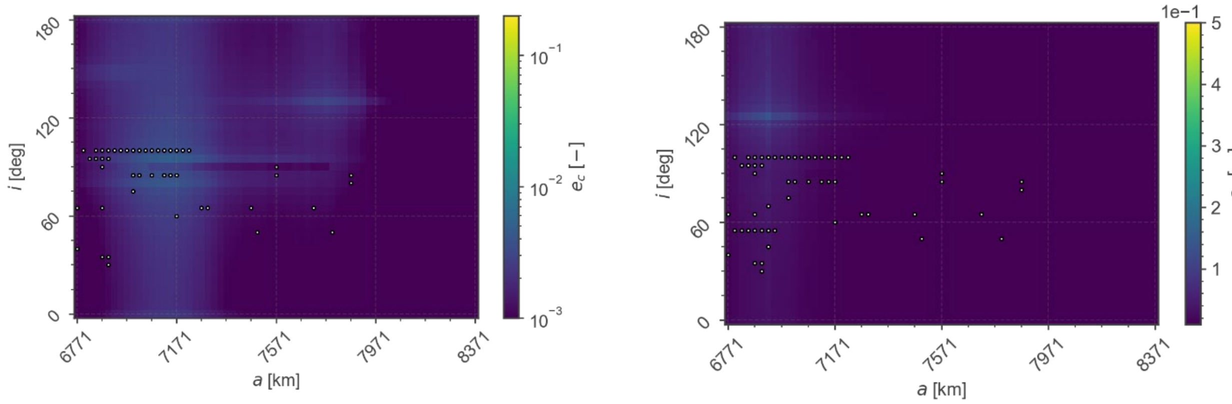

a) Collision effect maps in LEO with $\Delta t = 1$ year.

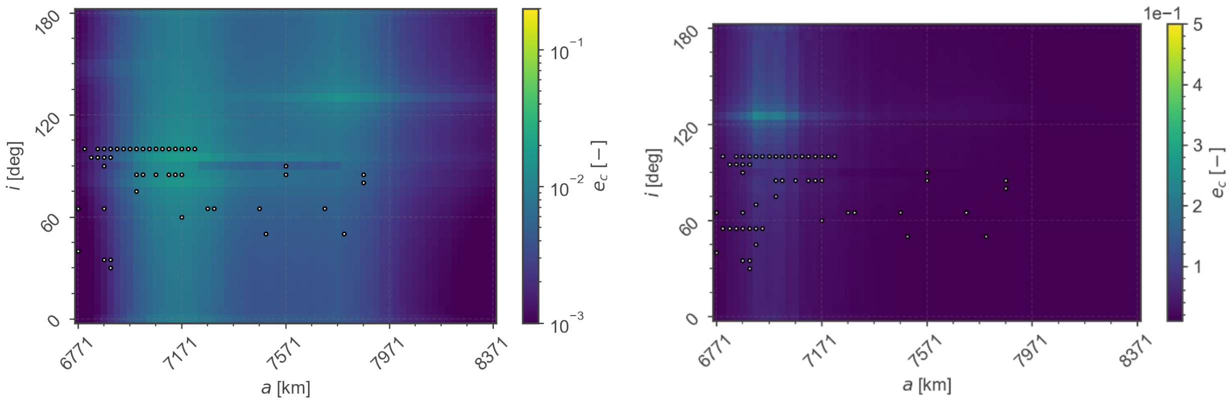

b) Collision effect maps in LEO with $\Delta t = 5$ years.

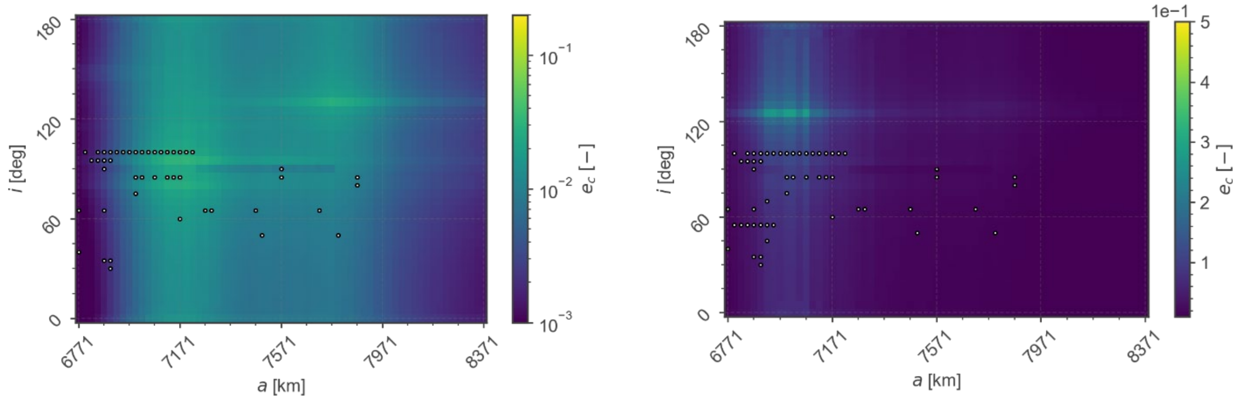

c) Collision effect maps in LEO with $\Delta t = 10$ years.

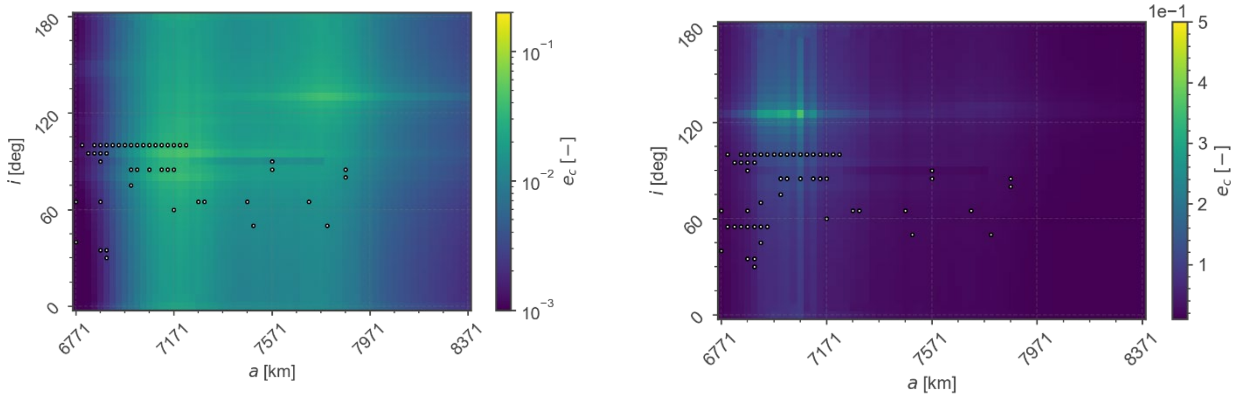

d) Collision effect maps in LEO with $\Delta t = 15$ years.

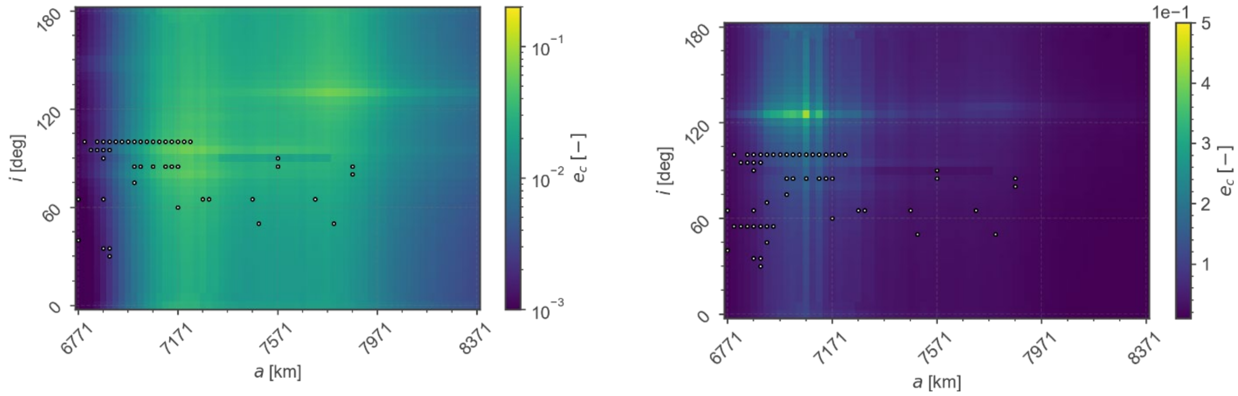

e) Collision effect maps in LEO with $\Delta t = 25$ years.

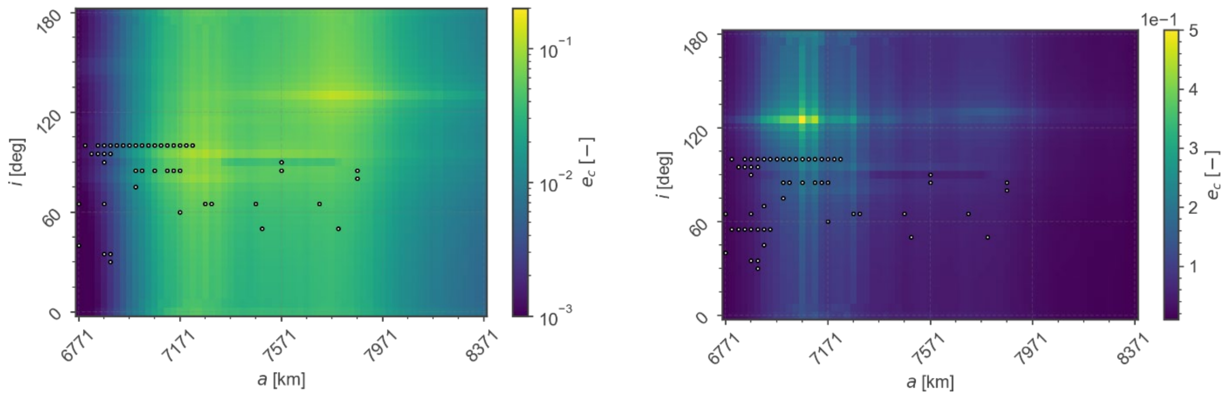

f) Collision effect maps in LEO with $\Delta t = 50$ years.

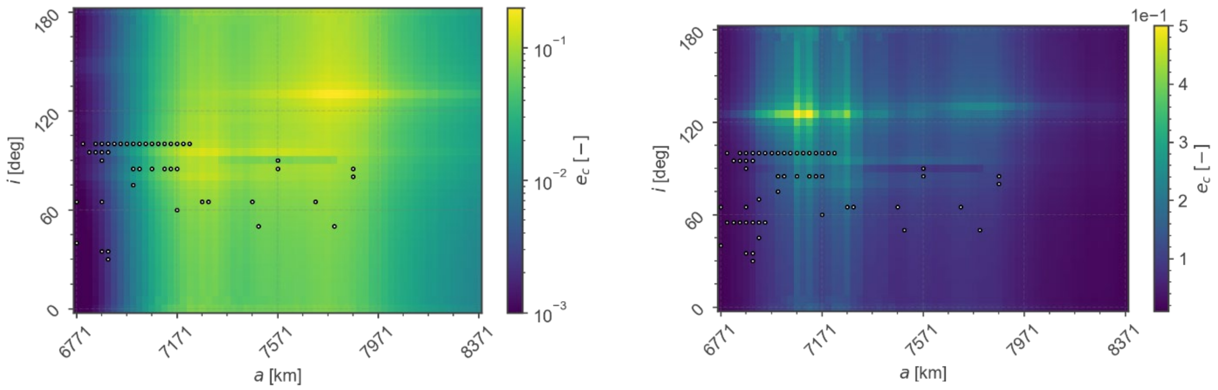

g) Collision effect maps in LEO with $\Delta t = 100$ years.

Figure 1. Collision effect maps in LEO for different times of debris cloud propagation. The white dots are representative targets position, not including (left column) and including the Starlink constellation (right column).

Effect maps without Starlink. When considering 1 year of propagation, the highest severity is observed at low altitudes, with a significant peak in the region "opposite" to the inclination of Sun-Synchronous Orbits (SSO) due to the high number of satellites in SSO and since the worst fragmentation that affect them is the head-on collision generated at $\pi - i_{SSO}$ [10]. Many fragments from previous collisions or explosions have not yet re-entered, and the affected region is densely populated. At higher altitudes, the peak effect is less pronounced compared to the lower altitudes due to the relatively short accumulation of debris and the initial lack of fragment re-entry.

As time progresses, the peak at low altitudes gradually diminishes. This trend is because the effects of debris cloud propagation do not account for additional fragmentations over time. Fragments at lower altitudes experience increased drag and re-enter the atmosphere, reducing their impact. However, the peak at higher altitudes grows in relative importance as the fragments remain in orbit longer, leading to a larger cumulative effect. As expected, the severity on the environment increases with the simulation time.

The crowded low LEO region experiences a substantial impact from any fragmentation, but since objects at low altitudes decay more quickly, the debris effects in this region are less persistent compared to higher altitudes. Objects in high LEO, on the other hand, exhibit longer residency times, which means their debris cloud remains in orbit for a longer duration. As the time of debris cloud propagation increases, this contributes more significantly to the overall effect, with the turnover for peak position occurring at 10 years for explosion effects and 25 years for catastrophic collisions (Figure 1e). The latter causes larger, faster-moving fragments, which contributes more significantly over time.

Effect maps with Starlink. The presence of Starlink significantly affects the severity of potential fragmentation events, with a peak occurring at slightly higher altitudes and "opposite" orbital inclinations compared to the constellation's objects. Starlink's low-altitude presence increases the overall collision probability, particularly for Starlink itself, as its large cross-sectional area makes it more vulnerable. As the time of debris cloud propagation increases, the high LEO region becomes increasingly important due to the longer residency time of debris, even if this effect is less pronounced than the cases without Starlink. In contrast, the low-altitude region reaches a saturation point, with the fragment cloud re-entering within the considered time frame, thus limiting the effect at lower altitudes as time progresses.

As the time interval extends, the peak severity shifts to higher altitudes, and the severity associated with the low-altitude peak (which would occur without Starlink) increases in importance as the analysed time grows, since a cloud of fragments at Starlink's altitude would re-enter more quickly, affecting the environment's severity at higher altitudes over time.

In conclusion, the analysis highlights how both time and orbital altitude significantly influence the severity of debris cloud effects, with Starlink's presence playing a pivotal role in shifting peak severity region in the map and extending the time over which these effects are significant. Based on these analysis we can conclude that propagation times of 10, 15, and 25 years are a good compromise to capture the key effects highlighted by the study, while balancing the trade-offs between the short-term and long-term debris cloud propagation impacts.

2.2 Impact of the time of debris cloud propagation on the population ranking

Additional analyses were conducted to explore the use of THEMIS as a mean for comparing the environmental impact of the many objects orbiting Earth, identifying those with the greatest impact similarly to what is done in [11].

A reference population from 2018 computed by A. Rossi with SDM [12] is considered, only active objects were considered for this analysis, and the environmental impact index is calculated for each object within the population, allowing for a ranking based on their environmental effect. Figure 2 illustrates the index values for the top 10 ranked objects according to the THEMIS metric without (left) and with (right) the inclusion of the Starlink constellation.

In the absence of Starlink, the highest-ranked objects are all near the low-altitude peak, with the Envisat satellite consistently ranking first. However, as propagation time increases, the low-altitude peak becomes less significant, allowing satellites further from the Sun-synchronous region to enter the top rankings.

With Starlink included, Envisat remains the highest-ranked object, but the top-ranked satellites now orbit closer to the Starlink-generated high effect peak. The propagation times considered are not long enough for the residency time of satellites in orbit to outweigh the impact of the severity peak in the low-altitude region. The top ten list remains quite similar for propagation times of 10, 15, and 25 years. Furthermore, the differences in index values between the various propagation times become less significant as the index values decrease. In conclusion, the presence of Starlink alters the positioning of objects in the ranking, with a notable shift toward high-peak altitudes of the maps with Starlink, though Envisat remains the highest-ranked object. Longer propagation times reduce the impact of the low-altitude peak, allowing for more variation in the top rankings.

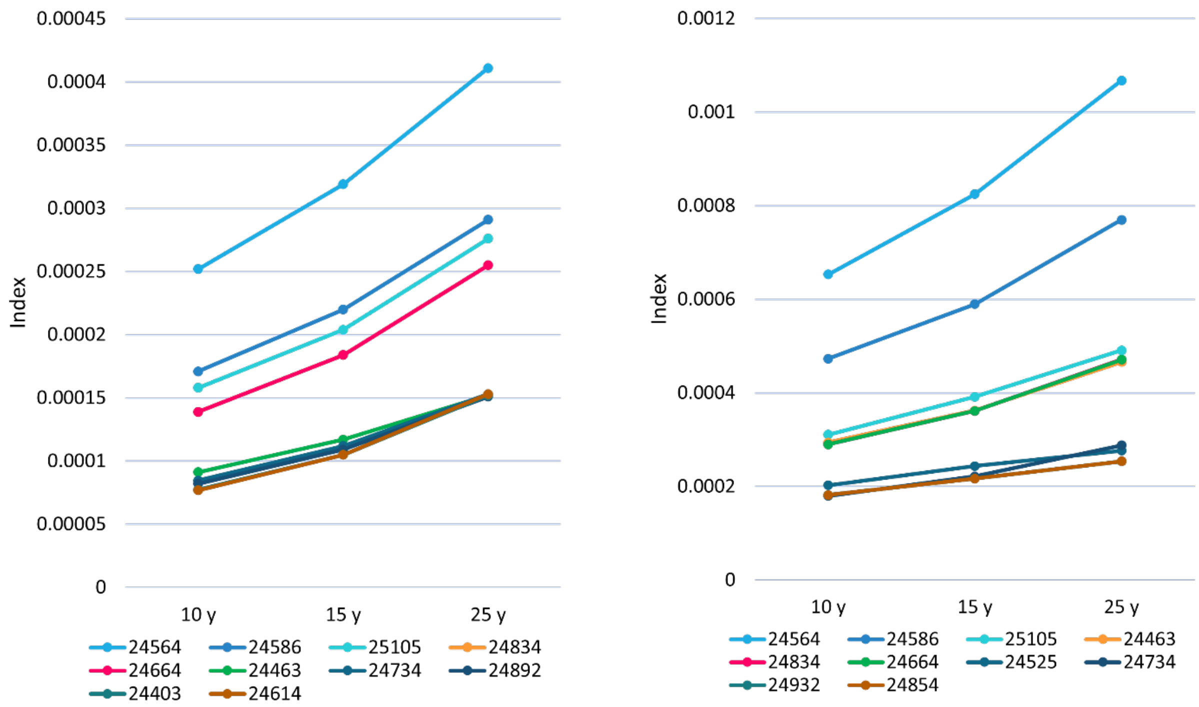

a) Index comparison with effect maps excluding Starlink.

b) Index comparison with effect maps including Starlink.

Figure 2. Index comparison with different Δt for the 10 top ranked objects according to THEMIS with Δt=15 years, not including (left column) and including (right column) the Starlink constellation.

2.3 Update frequency of targets population

As explained in Section 2, in THEMIS the severity terms are calculated with respect to a population of representative targets, which represent the active objects in space. Consequently, the effect defines the augmented risk due to an object breakup within a specific region, relative to other objects orbiting Earth. The targets are provided as a CSV file containing the Keplerian elements of the map bins where each representative object is located, along with its average and total areas. These targets are computed using data from the DISCOS database of in-orbit objects, following the methodology described in [14][15].

The software includes an option for expert users to update the population of representative targets by triggering a recalculation of the DISCOS population within the desired time range of stored data. For general users, however, the population of targets is fixed and updated by the administrators. The frequency of target updates influences how well the target population reflects the actual distribution of objects in space at the time of the analysis

The independent trigger code for the re-computation of the effect maps is utilised. This process requires a reference DISCOS population or any reference population, from which representative targets are computed. These targets are determined based on the minimum level of cross-sectional area approach outlined in [2], and they are selected from the objects on orbit within a user-defined time range.

The investigated alternatives for the update frequency of the target population are as follows:

- Fixed time-based update frequency: a yearly update, either manually or automated, could be implemented to trigger map updates at a fixed interval. Each year, the latest DISCOS population of active objects would be used to recompute the effect maps, which would then be the default in THEMIS for general use throughout the following year.
- Update frequency based on relevant parameters: this approach ties the update frequency to significant changes in the representative targets' definition, such as the appearance of a new target in a new position or a change in the total area of the population.

The analyses were carried out as described in the following. The DISCOS population's yearly changes were examined from 2014 to 2023. Following this, the impact of the different update criteria on the effect maps and index values was assessed for the years leading up to and beyond 2023. The results are presented in terms of the changes observed in the effect maps with different target populations and the impact these changes have on the index value for a set of analysed missions.

Table 1 presents the yearly statistics of changes in the LEO representative targets' population from DISCOS data between 2014 and 2023. These statistics include the introduction of new targets, the disappearance of previous ones, and changes in target area. The evolution of the LEO effect term over the years is shown in Figure 3.

Table 1. LEO representative targets yearly statistics from 2014 to 2023. The columns provide for each year the number of removed and added targets, the number of targets whose total area has changed, the total area change of the representative population as absolute and percentage values.

Update year	Removed objects	Added objects	Objects with total area change	Total area change [m²]	% of total area change
2015 vs 2014	0	3	13	369.7192	24.48254
2016 vs 2015	0	0	0	0	0
2017 vs 2016	0	2	11	301.1761	16.02125
2018 vs 2017	0	4	8	720.7076	33.04437
2019 vs 2018	0	4	14	709.9486	24.46633
2020 vs 2019	0	3	11	885.1332	24.50748
2021 vs 2020	0	7	15	9853.101	219.1127
2022 vs 2021	0	7	15	13785.43	96.06624
2023 vs 2022	0	8	25	23389.95	83.13367

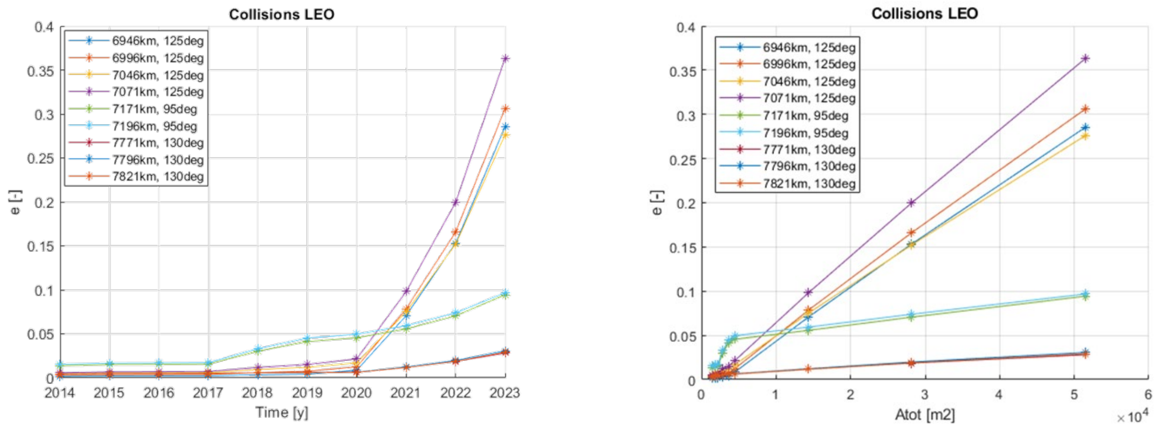

a) Collisions effect in LEO for different orbits computed with the representative targets' populations from 2014 to 2023.

b) Collisions effect in LEO for different orbits computed with the total area of the representative targets' populations from 2014 to 2023.

Figure 3. LEO effect evolution (a) with the various representative targets' populations from 2014 to 2023 for different LEO orbits, and (b) with the total area of the representative targets' populations from 2014 to 2023

3 DESIGN OF THE IMPLEMENTATION CHANGES FOR THEMIS 2.0

In parallel to the sensitivity analysis, the design of the implementation changes of the THEMIS tool has been defined. The original version of the software tool, as developed within the previous ESA-funded activity *"*S1-SC-01 – Design, development, and deployment of software infrastructure to assess the impact of a space mission on the space environment", is denoted as THEMIS 1 [1], while the new version from activity S2-SD-02 is called THEMIS 2. The design and implementation changes in THEMIS stem from two main sources: 1) update the software tool architecture to a virtualisation-based architecture, easing deployment, maintenance and future parallelization; and 2) cover the gaps in the software identified during the sensitivity analysis described in Section 2.

The architectural and code changes required to adapt the THEMIS back-end architecture and code to a new virtualised and containerised solution are described here.

To enable automatic deployment of THEMIS 2 in a virtualised environment, modifications to the back-end and THEMIS core architecture are required to clearly separate the front-end and back-end components. Other set of architectural changes required to adapt THEMIS to a virtualised and Dockerised solution, includes identifying and updating the external tools required by the software. An architecture where each tool is made available through a dedicated Docker container is preferred, as well as mitigating the restrictions on the Python version imposed by different dependencies of the THEMIS computational core. The following requirements are defined:

- ESA software dependencies (DMF, DELTA, DISCOS) shall run as separate containers, to simplify deployment and version update.
- Version compatibility restrictions between Python and Matlab Runtime (required by the PlanODyn propagator used within Starling) shall be mitigated.
- Matlab Runtime shall run as a separate container.
- The most time-consuming tasks (i.e., cloud propagation, impact estimation) shall have a code workflow that allows for node parallelization.
- Number and dimension of datafiles shall be reduced, for efficient data transfer during parallelisation and historical data storage.

Figure 4 provides a schematic representation of the updated architecture for the THEMIS back-end and core. The block in orange gathers the elements that were part of the core in THEMIS 1, which is now separated in 3 dedicated containers for the external tools (DMF, DELTA, PlanODyn) and one container for the Python elements of the core.

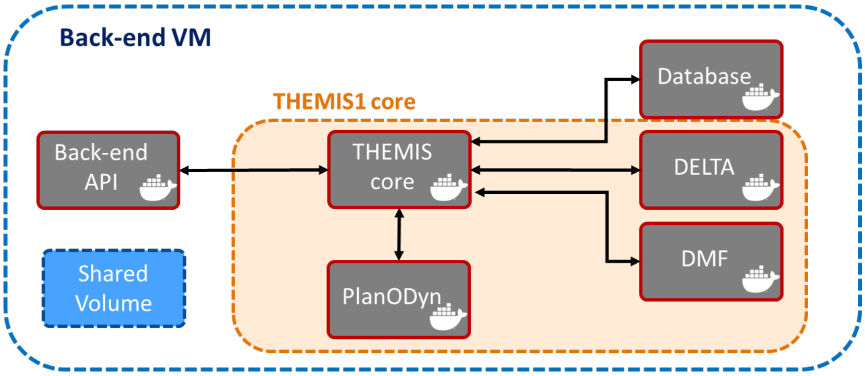

Figure 4. Updated architecture of the back-end and THEMIS core.

4 BETA TESTING PHASE FOR THEMIS 1.0

The THEMIS 1.0 version of the software is deployed at Politecnico di Milano servers, so the app is now accessible at https://themisweb.aero.polimi.it and requires a registration to the ESA Space Debris Office's Space Debris User Portal. In April 2025, 25 selected Beta testers among space debris experts, satellite operators and regulators will start the Beta testing phase, including some guided exercises to experience the THEMIS capabilities for the existing missions view, the planned mission analyses, the mission's detail page, the environmental impact evaluation, and the mission output view. The aim of the Beta testing phase is to collect feedback and other requests for further development to enhance the software's applicability and to start the process of integration of THEMIS 2.0 in other services such as possibly the Space Sustainability Rating and the Italian Space Agency IHS infrastructure.

Figure 5. THEMIS frontend landing page.

5 CONCLUSION

The sensitivity analyses and the deployment for the THEMIS software for "Tracking the Health of the Environment and Missions in Space" have been presented. Current work is performed to assess the influence of the software settings on the index computation. The resulting effect maps and index values are then compared. Then, the design of the implementation changes for THEMIS 2.0 are described and the Beta testing phase is presented and kicked off.

6 ACKNOWLEDGEMENT

This project has received funding from the European Space Agency contract ESA Contract No. 4000145375/24/D/BL. Potential users interested in becoming Beta testers can register their interest at:

https://forms.office.com/e/vD5H9Mp2YK

7 REFERENCES

[1] Colombo C., Muciaccia A., Giudici L., Gonzalo J.L., Masat A., Trisolini M., Del Campo B., Letizia L., Lemmens S., “Tracking the health of the space debris environment with THEMIS”, Aerospace Europe Conference 2023, 10th EUCASS – 9th CEAS, July 2023.

[2] Muciaccia A., Trisolini M., Giudici L., Colombo C., Del Campo B., Letizia F., "Environmental impact of large constellations through a debris index analysis", 73rd International Astronautical Congress (IAC), September 2022.

[3] Rusconi M., Muciaccia A., Gonzalo J. L., Colombo C. Letizia F., "Sensitivity analysis of THEMIS index configuration options for mission design applications", 11th European Conference for AeroSpace Sciences (EUCASS), 30 Jun. - 4 Jul., Rome, 2025.

[4] Colombo C., Trisolini M., Gonzalo J.L., Giudici L., Frey S., Kerr E., Sánchez-Ortiz N., Del Campo B., Letizia F., Lemmens S., “Assessing the impact of a space mission on the sustainability of the space environment”, 72nd International Astronautical Congress, 25-29 October 2021, Dubai.

[5] Colombo C., Trisolini M., Muciaccia A., Giudici L., Gonzalo J. L., Frey S., Del Campo B., Letizia F., Stijn L., “Evaluation of the Space capacity share used by a mission”, 73rd International Astronautical Congress, 18-22 September 2022, Paris, France, paper number IAC-22-A6.4.1.

[6] Colombo C., Giudici L., Muciaccia A., Gonzalo J.L., Del Campo B., Vyavahare N., Dutra D., Letizia F., Lemmens S., “Assessment of the collision risk in orbital slots and the overall space capacity”, IOC Conference 2023, Sugarland, Houston, USA

[7] Letizia F., Colombo C., Lewis H.G., Krag H., "Extending the ECOB Space Debris Index with Fragmentation Risk Estimation", 7th European Conference on Space Debris, ESA/ESOC, Darmstadt, Germany, 18-21 Apr. 2017.

[8] Johnson N.L., Krisko P. H., “NASA's new breakup model of EVOLVE 4.0,” Advances in Space Research, Vol. 28, Issue 9, pp. 1377–1384, 2001, doi: 10.1016/S0273-1177(01)00423-9.

[9] Giudici L., Trisolini M., Colombo C., “Probabilistic multi-dimensional debris cloud propagation subject to non-linear dynamics”, Advances in Space Research, Vol. 72, pp. 129-151, 2023.

[10] Giudici L., Gonzalo J.L., Colombo C., "Density-based in-orbit collision risk model valid for any impact geometry", Acta Astronautica, Vol. 219, 2024, pp. 785-803, https://doi.org/10.1016/j.actaastro.2024.03.067.

[11] McKnight D., Witner R., Letizia F., Lemmens S., Anselmo L., Pardini C., Rossi A., Kunstadter C., Kawamoto S., Aslanov V., Dolado Perez J-C, Ruch V., Lewis H., Nicolls M., Jing L., Dan S., Dongfang W., Baranov A., Grishko D.,"Identifying the 50 statistically-most-concerning derelict objects in LEO", Acta Astronautica, Vol. 181, 2021, pp. 282-291,https://doi.org/10.1016/j.actaastro.2021.01.021.

[12] Letizia F., Colombo C., Rossi A., Muciaccia A., Giudici L., Harada R., Kawamoto S., Böttcher L., Ruch V. Tallian C., “Mission-based and environment-based approaches for assessing the severity of a space debris evolution scenario from a sustainability perspective”, International Astronautical Congress, 2024, Milano, Italy.

[13] Giudici L., Gonzalo J.L., Muciaccia A., Colombo C., Trisolini M., Letizia F., "Environmental impact of object breakup in medium-Earth orbit", Advances in Space Research, 2024, DOI: 10.1016/j.asr.2024.06.012

[14] Giudici L., Gonzalo J.L., Muciaccia A., Colombo C., Trisolini M., Letizia F., “Environmental impact of object breakup in medium-Earth orbit, Advances in Space Research”, Vol. 74, Issue 4, 2024, pp. 1900-1915, https://doi.org/10.1016/j.asr.2024.06.012.

[15] Muciaccia A., Giudici L., Colombo C., “Space Environment Investigation Using a Space Debris Index”, 9th Annual Space Traffic Management Conference, 2023.